

The Pentacyanocyclopentadienyl System: Structures and Energetics

Richard L. Lord, Steven E. Wheeler, and Henry F. Schaefer III*

Center for Computational Chemistry, University of Georgia, Athens, Georgia 30602-2556

Received: March 30, 2005; In Final Form: July 13, 2005

In light of the recent silylation route to protonated pentacyanocyclopentadienyl (PCCp) anion reported by Richardson and Reed (Richardson, C.; Reed, C. A. *Chem. Commun.* **2004**, 706.), PCCp anion, neutral radical, and protonated species have been investigated theoretically. The predicted adiabatic electron affinity for PCCp (ZPVE-corrected value in parentheses) is enormous, 5.56 (5.47) eV. As with the unsubstituted cyclopentadienyl radical, the PCCp radical exhibits a Jahn–Teller distortion from the D_{5h} symmetry of the aromatic anion, yielding five equivalent 2B_2 minima that should show uninhibited pseudorotation about a D_{5h} conical intersection. Formation of the conjugate acid occurs via protonation of the anion at a nitrile nitrogen, which is favored over protonation at a ring carbon by 6.5 kcal/mol, with the preference explained by retention of aromaticity upon protonation at the nitrogen. Possible acid dimer structures have been investigated to evaluate the proposed polymeric acid structure of Richardson and Reed. Our predictions confirm their suggested polymeric structure, but we also present an alternative, self-contained dimer that should be competitive kinetically and thermodynamically. Vibrational frequencies and infrared intensities are predicted, to aid in the experimental identification of several of these species.

Introduction

The pentacyanocyclopentadienide (PCCp) anion has fascinated chemists since it was first synthesized by Webster in the mid 1960s.^{1,2} The stability and low nucleophilicity of this anion, ascribed to delocalization and aromaticity, allows its classification as a weakly coordinating anion. Applications of weakly coordinating anions and the corresponding conjugate acids include, but are not limited to, counterions of catalysts in polymer reactions, crystallization reagents, and electrolytes in nonaqueous or aprotic media.^{3,4}

The PCCp anion was long thought to be unprotonatable after unsuccessful attempts with many different acids, including the strong perchloric oxyacid.² The recent report by Richardson and Reed,⁵ however, shows that silylation followed by exposure to triflic acid in toluene precipitates the elusive acid. Based on solubility tests, a lack of cyclopentadiene-like IR bands consistent with protonation of a ring carbon, and the absence of characteristic infrared N–H stretching bands near 3000 cm^{-1} , they describe the acid as being polymeric, depicted in Figure 1, with short, strong, low-barrier (SSLB)⁶ N–H–N bonds.

Over the past fifteen years the PCCp anion has been studied with a number of theoretical methods.^{7–11} While it is commonly accepted that the aromatic anion maintains D_{5h} symmetry, confirmed by experiment in 1973,¹² a recent paper by Tang et al. reports C_{2v} symmetry.⁹ However, the geometry presented by Tang et al. actually exhibits D_{5h} symmetry, not C_{2v} . Johansson et al. investigated complexes of Li^+ with the PCCp anion and other heterocyclic anions,¹⁰ while Koppel and co-workers^{7,8} have carried out a series of studies on the gas-phase acidities of a number of superacids, including the PCCp anion and its conjugate acid, using semiempirical (PM3) and density functional (B3LYP) methods. The 6-311+G** B3LYP deprotonation energy,⁸ without ZPVE corrections, was 256.6 kcal/mol. However, they appear to have only studied protonation

of a ring carbon (to form pentacyanocyclopentadiene) and do not report relative energies of alternate protonated structures. Recently, Vianello et al. investigated neutral organic superacids formed from cyclopentadiene derivatives. Their study included both nitrile nitrogen and ring carbon protonated PCCp–H isomers with respective ZPVE-corrected deprotonation enthalpies of 263.5 and 256.5 kcal/mol at the B3LYP/6-311+G(d,p)//B3LYP/6-31G(d) level of theory.¹¹

In the current research, we examine the anion and neutral structures, along with adiabatic electron affinities (EA_{ad}), vertical electron affinities (EA_{vert}), and vertical detachment energies (VDE), using three carefully calibrated density functional theory (DFT) methods.¹³ We also explore potential conjugate acid structures and model the dimerization of two protonated pentacyanocyclopentadienide anions to evaluate the suggested polymeric structure of Richardson and Reed.⁵ Further, we characterize the potential energy surface along the N–H stretching mode to investigate the presence (or absence) of SSLB hydrogen bonds and to aid in the interpretation of IR spectra.

Theoretical Methods

The basis set chosen for this study is described in the recent review by Rienstra-Kiracofe et al.¹³ This set, herein denoted DZP++, comprises the standard Huzinaga–Dunning double- ζ basis set^{14,15} with additional pure spherical harmonic polarization functions [$\alpha_{\text{p}}(\text{H}) = 0.75$, $\alpha_{\text{d}}(\text{C}) = 0.75$, $\alpha_{\text{d}}(\text{N}) = 0.8$] and additional diffuse functions [$\alpha_{\text{s}}(\text{H}) = 0.04415$, $\alpha_{\text{s}}(\text{C}) = 0.04302$, $\alpha_{\text{p}}(\text{C}) = 0.03629$, $\alpha_{\text{s}}(\text{N}) = 0.06029$, $\alpha_{\text{p}}(\text{N}) = 0.05148$]. The neutral PCCp radical, the PCCp anion, and the protonated structure PCCp–H were modeled using this DZP++ basis set, while the dimer structures were optimized using the same basis set excluding the diffuse functions, denoted DZP.

Three different DFT functionals were utilized: Becke's three-parameter functional¹⁶ with Lee, Yang, and Parr's correlation functional¹⁷ (B3LYP); Becke's 1988 exchange functional¹⁸ with Perdew's 1986 correlation functional^{19,20} (BP86); and Becke's

* Corresponding author: hfs@uga.edu.

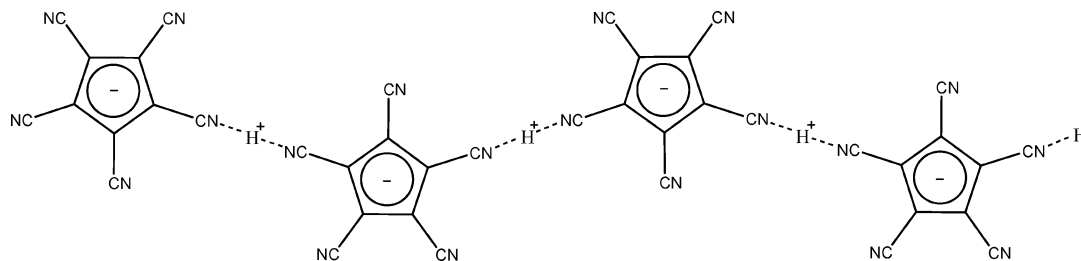


Figure 1. Polymeric acid structure proposed by Richardson and Reed (ref 5).

1988 exchange functional with Lee, Yang, and Parr's correlation functional (BLYP). These three functionals, combined with the DZP++ basis set, have been shown to accurately predict experimental electron affinities for a test set of 91 atoms and molecules. For this test set, the B3LYP, BLYP, and BP86 results exhibited average errors of 0.14 (0.16), 0.14 (0.15), and 0.18 (0.19) eV, respectively, where harmonic zero-point vibrational energy (ZPVE) corrected average errors are listed in parentheses.¹³ These errors are on par with or smaller than experimentally observed errors for all but a few molecules. More specifically, Rienstra-Kiracofe et al.²¹ demonstrated excellent agreement between experimental^{22,23} and DFT values for the electron affinity of cyclopentadiene, with BP86 performing the best among these three.

Investigations were carried out using the Q-Chem 2.1 computational chemistry package.²⁴ Convergence thresholds for geometry optimizations were 15×10^{-6} hartree bohr⁻¹ for gradients, 60×10^{-6} bohr for displacements, and 1×10^{-6} hartree for the energy. Analytically computed harmonic vibrational frequencies were used to characterize each stationary point and to provide ZPVE corrections. All structures presented herein are minima unless otherwise stated. The adiabatic electron affinity (EA_{ad}), vertical electron affinity (EA_{vert}), vertical detachment energy (VDE), and deprotonation energy (DE) are defined explicitly:

$$EA_{ad} = E_{(optimized\ neutral)} - E_{(optimized\ anion)}$$

$$EA_{vert} = E_{(optimized\ neutral)} - E_{(anion\ at\ neutral\ geometry)}$$

$$VDE = E_{(neutral\ at\ anion\ geometry)} - E_{(optimized\ anion)}$$

$$DE = E_{(optimized\ anion)} - E_{(optimized\ protonated\ structure)}$$

To understand the energy differences between competing protonated structures, nuclear-independent chemical shift (NICS)²⁵ values have been determined as a gauge of aromaticity. NICS values were computed at the center of the ring (NICS0) for each of the acid structures using the DZP++ GIAO-B3LYP method,^{26–30} at optimized DZP++ B3LYP geometries, using Gaussian94.³¹

Results and Discussion

The following discussion will utilize the standard IUPAC numbering scheme for a substituted Cp ring, with carbon 1 along the C_2 axis in the C_{2v} neutral radical and the ring carbon closest to the protonation site for the conjugate acids. Carbon atom numbers are included in the figures for clarity.

I. PCCp Anion and Its Electron-Detached Neutral Radical. Geometries for the anion and the 2B_2 neutral radical are shown in Figures 2 and 3, respectively, optimized using the B3LYP, BLYP, and BP86 methods with the DZP++ basis set. The aromatic pentacyanocyclopentadienide anion exhibits D_{5h} symmetry, with complete delocalization of the six π -electrons. However, the formation of the corresponding neutral radical

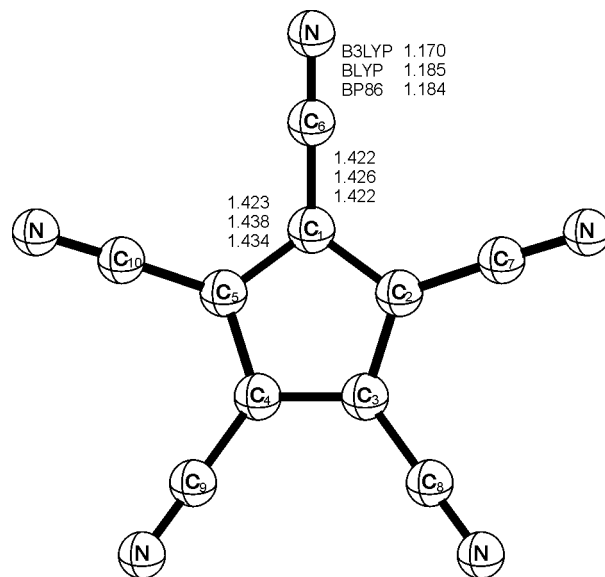


Figure 2. PCCp anion (D_{5h}) bond lengths (Å) optimized at the DZP++ B3LYP, BLYP, and BP86 levels of theory.

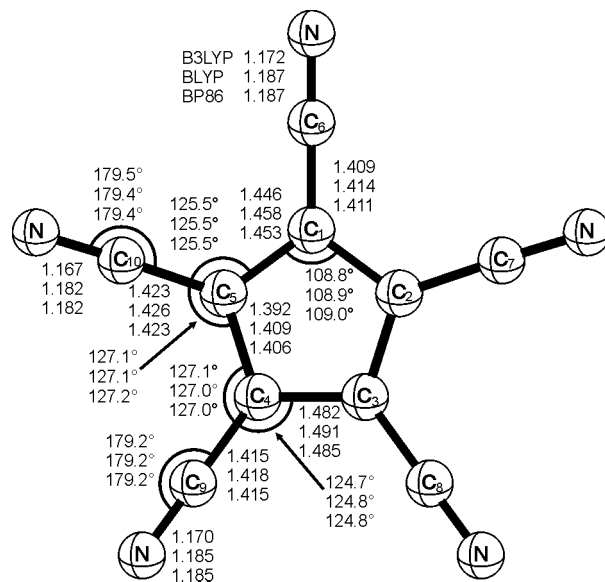


Figure 3. Structure of the 2B_2 component of the Jahn–Teller split PCCp neutral radical (C_{2v}), optimized at the DZP++ B3LYP, BLYP, and BP86 levels of theory (bond lengths are in Å).

yields a ${}^2E_1'$ state that will distort to C_{2v} or lower symmetry due to the Jahn–Teller effect.

We have investigated the resulting 2A_1 and 2B_2 structures using DZP++ B3LYP, and the harmonic vibrational frequencies suggest that the 2B_2 structure (Figure 3) is a minimum. The distorted 2A_1 structure (Figure 4) corresponds to a transition state separating equivalent 2B_2 structures (there will, of course, be five equivalent 2B_2 minima separated by five equivalent 2A_1

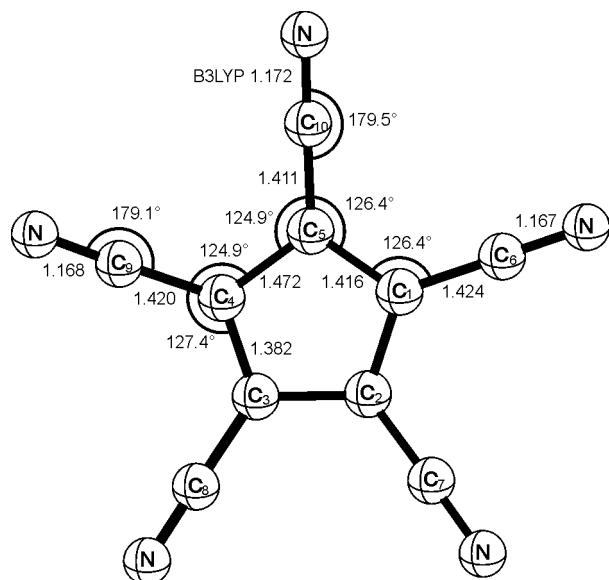


Figure 4. Structure of the 2A_1 component of the Jahn–Teller split PCCp radical (C_{2v}), optimized at the DZP++ B3LYP level of theory (bond lengths are in Å). This structure corresponds to the transition state for pseudorotation, connecting equivalent forms of the 2B_2 structure, shown in Figure 3.

TABLE 1: Electron Affinities (eV) of PCCp (ZPVE-Corrected Values in Parentheses)

	B3LYP	BLYP	BP86
EA _{ad}	5.56 (5.47)	5.26 (5.18)	6.05 (5.97)
EA _{vert}	5.44	5.17	5.97
VDE	5.68	5.34	5.60

transition state structures). Given the minor differences in geometry between the 2B_2 and 2A_1 geometries, it is not surprising that the computed barrier to pseudorotation, through the 2A_1 transition state, is negligible (<0.01 kcal). The resulting picture is one of uninhibited pseudorotation about a D_{5h} conical intersection, similar to the potential energy surface of the Cp radical.^{21,32,33} Applegate et al. argued,³⁴ based on symmetry, that the energy should be invariant with respect to the pseudorotation coordinate for the Cp ring. Given the expected precision of DFT integration grids and the energy convergence criterion utilized for optimizations, this suggestion is consistent with our results. Regardless, since our current focus is on the electron affinity of this radical, we have computed only the 2B_2 C_{2v} minimum with the remaining functionals.

In the neutral 2B_2 radical, the unpaired electron is largely localized on ring carbon C_1 , with spin density analysis indicating partial delocalization to the adjacent nitrile N and carbons C_3 and C_4 (see Figure 3 for numbering scheme). Such a distribution of spin density is expected from partial delocalization through the π -system. The geometry changes observed going to the neutral radical are a lengthening of the C_1 – C_2 and C_3 – C_4 bond lengths along with a contraction of the C_2 – C_3 bond length, consistent with a gain in cyclopentadiene character. The nitrile groups are relatively unaffected, with only slight deviations from linearity, except for the nitrile at C_1 , which experiences an elongation of the connecting C–C bond due to the disruption of resonance with the ring.

Computed EA_{ad} values, with ZPVE-corrected values in parentheses, are enormous, 5.56 (5.47), 5.26 (5.18), and 6.05 (5.97) eV using the B3LYP, BLYP, and BP86 functionals, respectively. With the use of these same functionals (the EA_{vert}, VDE) values are (5.44, 5.68), (5.17, 5.34), and (5.97, 5.60) eV, respectively. A summary of these electron affinities is shown

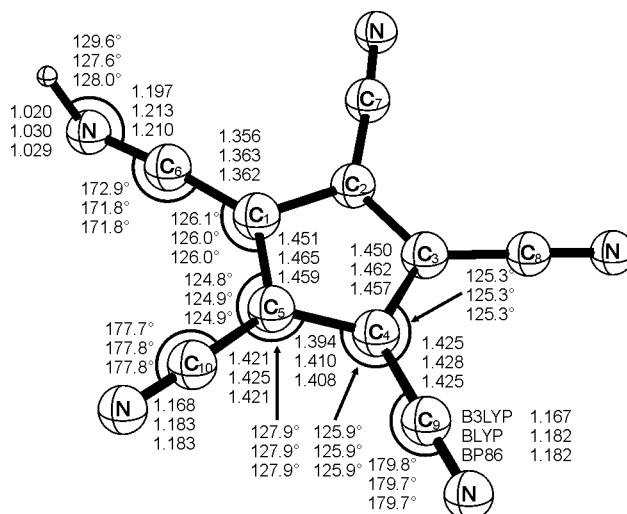


Figure 5. PCCp acid 1 (C_{2v}) bond lengths (Å) and angles, optimized at the DZP++ B3LYP, BLYP, and BP86 levels of theory.

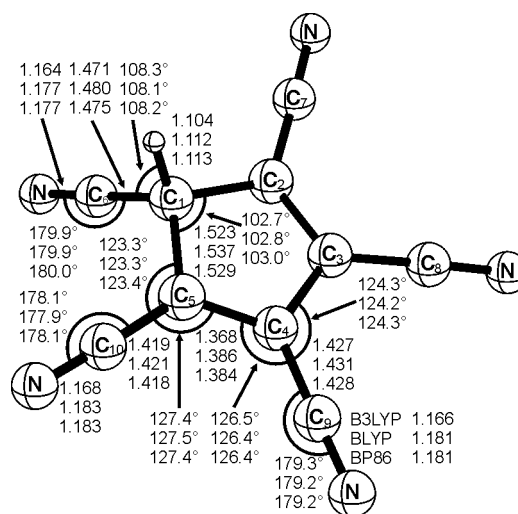


Figure 6. PCCp acid 2 (C_{2v}) bond lengths (Å) and angles, optimized at the DZP++ B3LYP, BLYP, and BP86 levels of theory.

in Table 1. The large EA values are expected, given the stabilization of the anion due to aromaticity coupled with the electron-withdrawing effect of the five cyano groups. The neutral radical is not aromatic and is not subject to as large a stabilization effect due to the cyano groups. The theoretical adiabatic EA of the unsubstituted Cp radical is 1.71 eV (using DZP++ B3LYP),²¹ less than one-third the magnitude of that for PCCp. To a crude approximation, the difference of 3.7 eV may be attributed to the stabilization of the PCCp anion afforded by the five cyano substituents, since the aromatic stabilization of the anion is expected to be of similar magnitude for the two systems. Irrespective of the interpretation, cyano substitution has a profound effect on the Cp radical and anion.

II. PCCp Conjugate Acids. Two distinct acid minima were located using all three DFT functionals, in agreement with the findings of Vianello et al.¹¹ The geometries for acid 1, with the proton bound to a nitrogen, and acid 2, with the proton bound to a ring carbon, are shown in Figures 5 and 6, respectively. We were unable to locate a stationary point corresponding to a proton bound to the cyano carbon. Natural population analysis³⁵ of the PCCp anion yields charges of -0.37 , $+0.33$, and -0.15 au on the nitrogens, cyano carbons, and ring carbons, respectively, consistent with our findings regarding the favored protonation positions. A summary of the deprotonation enthal-

TABLE 2: Deprotonation Enthalpies (0 K, kcal/mol), Corresponding to the Reaction $\text{PCCp-H} \rightarrow \text{PCCp}^- + \text{H}^+$

	B3LYP	BLYP	BP86	previous work ^b
acid 1	269.3 (262.5)	271.0 (264.4)	271.2 (264.7)	(263.5)
acid 2	262.8 (256.0)	263.1 (256.6)	262.1 (255.7)	(256.5)
energy difference	6.5 (6.5)	7.9 (7.8)	9.1 (9.0)	(7.0)

^a Also included are energy differences for the conjugate acid structures (ZPVE-corrected values in parentheses). ^b From ref 11, at 298 K.

TABLE 3: Harmonic Vibrational Frequencies (cm^{-1}) and IR Intensities (km/mol, in Parentheses) for Acid 1 (C_s Symmetry), Predicted Using the DZP++ B3LYP and BP86 Methods

B3LYP		BP86	
a'	a''	a'	a''
68 (4)	71 (0)	71 (5)	76 (0)
95 (0)	88 (4)	101 (0)	92 (4)
107 (7)	106 (1)	111(7)	111 (2)
110 (10)	227 (1)	115 (11)	235 (1)
232 (7)	235 (1)	242 (9)	246 (1)
416 (4)	411 (1)	433 (1)	432 (2)
422 (22)	421 (1)	438 (47)	435 (0)
453 (1)	462 (1)	471 (2)	482 (1)
475 (3)	495 (0)	488 (1)	578 (0)
478 (1)	527 (9)	497 (13)	551 (11)
493 (18)	629 (66)	513 (43)	651 (75)
538 (8)	755 (0)	564 (28)	789 (0)
713 (696)	774 (2)	683 (783)	814 (2)
725 (41)	847 (3)	764 (3)	868 (3)
862 (10)	1145 (5)	855 (7)	1177 (6)
1170 (17)	1348 (3)	1201 (26)	1394 (4)
1348 (21)	1494 (1)	1386 (50)	1560 (2)
1412 (54)	2211 (31)	1457 (82)	2315 (43)
1454 (9)	2228 (2)	1506 (19)	2329 (1)
2109 (931)		2171 (1161)	
2213 (2)		2317 (4)	
2221 (2)		2325 (8)	
3475 (225)		3584 (345)	

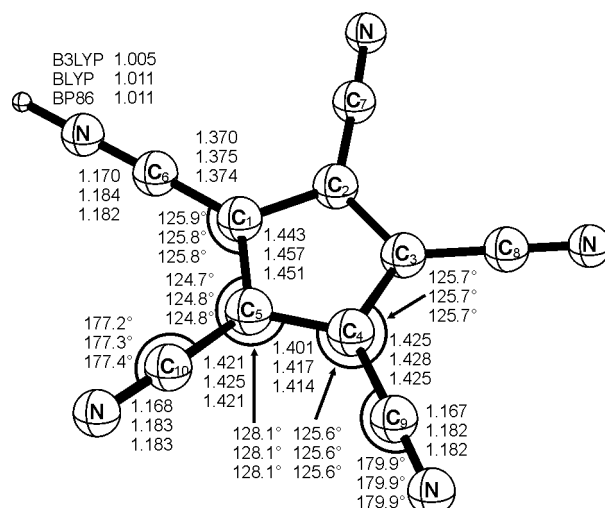
pies (0 K) and relative stabilities is included in Table 2. Predicted harmonic vibrational frequencies are included in Tables 3 and 4 for acids 1 and 2, respectively.

Acid 1 (C_s symmetry), a structure with a bent nitrile arm where the proton is bound to the nitrogen, has a barrier to inversion of 2.4 kcal/mol (using B3LYP) through a planar C_{2v} transition state structure, shown in Figure 7. The acid structure exhibits an elongation of the nitrile bond at the site of protonation as well as contraction of the connecting C–C bond length, relative to that of the anion. The resulting C–C bond length is 1.356 Å (using B3LYP), which is slightly longer than a typical (ethylene) C–C double bond. The other nitrile bond lengths are relatively unaffected, though a slight bending of these arms is observed. The qualitative changes of the ring bond lengths are the same as those seen upon formation of the neutral radical: elongation of the C_1 – C_2 and C_3 – C_4 bonds and a shortening of the C_2 – C_3 distance. The lengthening along C_3 – C_4 is of a much smaller magnitude than that observed for the neutral radical. The average difference in bond length between our reported structure and that of Vianello et al.¹¹ is 0.004 Å, with a standard deviation of 0.001 Å, well within the expected error of DFT. The theoretical gas-phase deprotonation enthalpies (ZPVE-corrected values given in parentheses) for this species are 269.3 (262.5), 271.0 (264.4), and 271.2 (264.7) kcal/mol using B3LYP, BLYP, and BP86, respectively. Our ZPVE-corrected B3LYP result (262.5 kcal/mol) compares well with the value of Vianello et al. (263.5 kcal/mol).

TABLE 4: Harmonic Vibrational Frequencies (cm^{-1}) and IR Intensities (km/mol, in Parentheses) for Acid 2 (C_s Symmetry), Predicted Using the DZP++ B3LYP and BP86 Methods

B3LYP		BP86	
a'	a''	a'	a''
54 (1)	74 (0)	49 (1)	71 (0)
101 (2)	95 (0)	96 (1)	91 (0)
104 (13)	112 (9)	100 (11)	107 (7)
115 (13)	224 (0)	111 (11)	215 (0)
222 (2)	243 (0)	212 (1)	233 (0)
344 (1)	404 (0)	328 (0)	388 (0)
430 (2)	428 (2)	414 (1)	415 (3)
445 (2)	459 (1)	430 (1)	440 (0)
466 (2)	487 (0)	453 (1)	467 (0)
488 (0)	551 (0)	469 (0)	529 (0)
515 (2)	731 (2)	497 (2)	703 (2)
629 (0)	795 (0)	604 (0)	761 (0)
760 (1)	848 (11)	728 (1)	825 (9)
913 (8)	1101 (7)	884 (6)	1071 (6)
1073 (1)	1159 (11)	1041 (1)	1111 (9)
1193 (1)	1328 (4)	1157 (1)	1283 (6)
1275 (0)	1640 (8)	1222 (0)	1565 (8)
1355 (9)	2314 (0)	1315 (6)	2207 (1)
1585 (0)	2337 (4)	1516 (0)	2235 (5)
2313 (1)		2206 (1)	
2334 (1)		2230 (3)	
2351 (0)		2252 (0)	
3033 (14)		2950 (11)	

The second acid minimum (C_s symmetry), with the proton bound directly to the ring carbon, is found to lie 6.5, 7.9, and 9.1 kcal/mol higher in energy than that of acid 1 using the B3LYP, BLYP, and BP86 functionals. Zero-point-corrected relative energies are 6.5, 7.8, and 9.0 kcal/mol, respectively, compared to the ZPVE-corrected energy of 7 kcal/mol computed by Vianello et al.¹¹ The B3LYP deprotonation energy for acid 2 is seen to agree with the value reported by Koppel et al.,⁸ and the ZPVE-corrected deprotonation energy agrees well with Vianello et al.¹¹ The elongation of the bond between the nitrile and ring carbon at the point of protonation, accompanied by a decrease in the C_5 – C_1 – C_2 angle to 103° , are indicative of a rehybridization of the ring carbon from sp^2 to sp^3 . This rehybridization also accounts for the lengthening of the C_1 – C_2 bond length and the shortening of the C_2 – C_3 bond length of greater magnitude than that seen in the neutral radical or

**Figure 7.** PCCp acid transition state (C_{2v}) bond lengths (Å) and angles, optimized at the DZP++ B3LYP, BLYP, and BP86 levels of theory. This transition state connects equivalent forms of acid 1, shown in Figure 5.

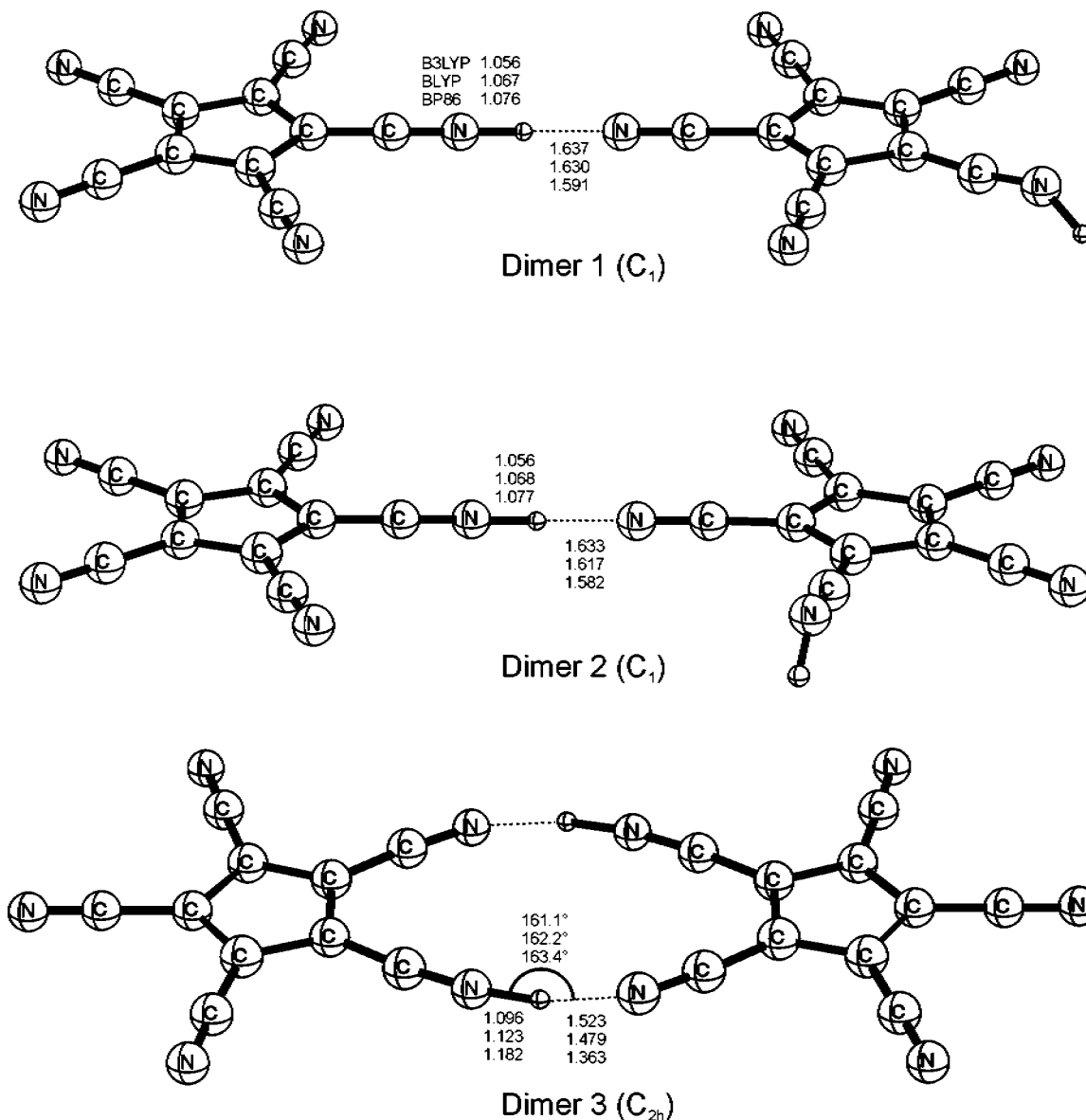


Figure 8. PCCp acid dimer bond lengths (Å) and angles, optimized at the DZP B3LYP, BLYP, and BP86 levels of theory.

acid 1. The other nitrile groups are mostly unaffected. Again, our geometry shows remarkable agreement with that of Vianello et al., having an average difference of 0.003 Å with a standard deviation of 0.002 Å.

The relative energies of the two acids, shown in Table 2, can be justified in terms of retention of aromaticity upon formation of acid 1, as measured by computed NICS values.²⁵ NICS values have been shown to correlate well with alternative measurements of aromaticity based on geometric, energetic, and other magnetic criteria,^{25,36–40} with a more negative NICS value indicative of greater aromaticity. The primary advantage of using NICS as a gauge of aromaticity is that no reference molecule or calibration is required,²⁵ yielding, in the limit of large rings, an absolute scale for aromaticity. The NICS values, calculated at the DZP++ GIAO-B3LYP level of theory, are -16.5 , -13.9 , and -7.90 ppm for the anion, acid 1, and acid 2, respectively. There is a slight disruption of aromaticity upon formation of acid 1, evinced by the slight increase in the NICS value of acid 1 compared to that of the anion, while acid 2 exhibits a more drastic reduction in aromatic character. Such a result is expected given the rehybridization of the ring carbon and concomitant disruption of the continuous ring of p-orbitals that accompanies

the formation of acid 2. Despite this extreme difference in aromatic character, both acids qualify as superacids. Therefore, while the aromaticity retention explains the relative energies of the acids well, the overwhelming acidity of these isomers is primarily due to the anion resonance effect and not aromaticity, as noted by Vianello et al.¹¹

III. PCCp Acid Dimers. To more directly evaluate the merits of the postulated protonated polymer structure of Richardson and Reed,⁵ we have computed optimized geometries for three plausible dimers of protonated PCCp, shown in Figure 8. Given the size of these structures and the relatively small changes that occur relative to the structure of isolated acid 1 upon dimerization, we have elected to include in Figure 8 only the optimized parameters for the N–H bonds. The first dimer (dimer 1), representing a segment of the polymeric arrangement suggested by Richardson and Reed, features a head-to-tail alignment with a proton asymmetrically bridging two cyano groups.

Clearly, there should exist a distinct isomeric structure (dimer 2) with the singly bound proton connected to the C_2 nitrile group, rather than the C_3 nitrile. Given the stereoelectronic equivalence of the C_2 and C_3 ring positions in a Cp system, we expect the energies of these two distinct structures to be nearly equal, and

TABLE 5: Dissociation Energies of Possible Acid Dimer Structures, Corresponding to Reaction 1 (ZPVE-Corrected Values in Parentheses)

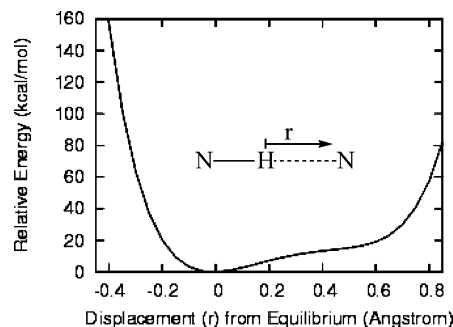
	B3LYP	BLYP	BP86
dimer 1	14.4 (12.3)	12.8 (10.8)	13.4 (11.4)
dimer 2	13.4 (11.3)	12.1 (10.2)	12.7 (10.8)
dimer 3	26.2 (24.6)	24.4 (23.6)	26.8 (27.4)

they were found to differ by only 1.01, 0.63, and 0.70 kcal/mol using B3LYP, BLYP, and BP86, respectively, including ZPVE corrections. However, polymer steric crowding, which is not accounted for in these calculations, may limit binding to the C₂ nitrile in an extended polymer. Additionally, there should be nearly uninhibited rotation about the N–H–N bonds in both dimers 1 and 2, imparting a large degree of conformational flexibility to the chain. Given the ability to bond to either the C₂ or C₃ nitrile positions, along with the possibility of introducing branching by joining multiple chains at a single PCCP ring, the resulting polymer would be expected to have a highly irregular, networked structure.

Since the characterization of the polymer structure by Richardson and Reed⁵ was partially based on the lack of the characteristic N–H stretching band, an alternative self-contained isomeric dimer structure (dimer 3, see Figure 8), was also investigated. Dimer 3 was predicted to lie 11.7, 11.5, and 13.4 kcal/mol lower in energy than dimer 1 using B3LYP, BLYP, and BP86, respectively. ZPVE-corrected energy differences for B3LYP, BLYP, and BP86 are 12.4, 12.8, and 15.9 kcal/mol. This energy ordering is expected, however, since dimer 3 is connected via two hydrogen bonds. Dissociation energies for all three dimers are included in Table 5, corresponding to the enthalpy (at 0 K) of the following reaction:



As seen in Table 5, the stabilization afforded by *each* hydrogen bond is nearly equal for all three dimers, suggesting that there is little or no ring strain introduced upon formation of dimer 3. For all three dimers considered, the N–H \cdots N hydrogen bond

**Figure 9.** Approximate potential energy curve along the N–H stretching coordinate for dimer 1, shown in Figure 8. The energy was computed at the DZP B3LYP level of theory for fixed monomer positions as a function of the displacement from the equilibrium N–H distance.

is seen to be asymmetric, though BLYP and BP86 predict smaller degrees of asymmetry than B3LYP. This is most pronounced in the case of dimer 3, for which BP86 predicts N–H and N \cdots H bond distances that differ by only 0.18 Å.

Despite the favorable dimerization energy of dimer 3, dimers 1 and 2 would be expected to more readily form a polymeric structure. Such a chain of PCCp–H moieties will have one fewer hydrogen bond than the corresponding number of isolated dimer 3 structures (e.g., four PCCp–H structures can join head-to-tail to form a continuous chain linked by three hydrogen bonds, as in Figure 1, compared to the same number of PCCp–H monomers joining to form two isolated dimer 3 structures, connected by a total of four hydrogen bonds). However, in the limit of an extended polymer, the resulting energy difference will become negligible and the thermodynamics, at finite temperature, will be dominated by entropic considerations. Regardless, the polymerization process should be controlled by kinetic factors, which strongly favor the formation of the doubly hydrogen-bound dimer.

We have also examined the discussion of Richardson and Reed⁵ concerning the existence of SSLB hydrogen bonds in dimer 1. Plotted in Figure 9 is an approximate potential energy

TABLE 6: Harmonic Vibrational Frequencies (cm⁻¹) and IR Intensities (km/mol, in Parentheses) for Dimer 1 (C₁ Symmetry), Predicted Using the DZP B3LYP and BP86 Methods^a

B3LYP				BP86			
32 (0)	424 (51)	555 (48)	1465 (48)	30 (0)	407 (18)	530 (16)	1424 (356)
39 (1)	429 (0)	623 (668)	1471 (668)	37 (1)	411 (0)	617 (69)	1439 (0)
70 (7)	433 (9)	644 (78)	1487 (78)	66 (6)	415 (5)	651 (808)	1449 (27)
73 (4)	435 (16)	722 (1)	1506 (1)	70 (0)	421 (20)	680 (0)	1456 (9)
74 (0)	436 (29)	731 (4)	1534 (4)	72 (4)	423 (14)	689 (12)	1475 (18)
78 (5)	439 (0)	748 (0)	1558 (0)	75 (4)	425 (0)	705 (0)	1496 (4)
95 (5)	452 (0)	753 (5)	2190 (5)	90 (4)	432 (0)	712 (5)	2127 (1266)
100 (0)	453 (23)	796 (0)	2266 (0)	96 (0)	439 (23)	761 (0)	2172 (38)
102 (0)	476 (18)	797 (1)	2308 (1)	97 (0)	459 (9)	761 (0)	2207 (88)
102 (3)	478 (1)	870 (0)	2311 (0)	98 (3)	461 (2)	848 (0)	2209 (5)
107 (2)	486 (6)	872 (4)	2315 (4)	102 (1)	467 (2)	850 (4)	2211 (21)
113 (11)	487 (12)	881 (33)	2316 (33)	108 (10)	468 (1)	859 (25)	2212 (2)
113 (14)	489 (3)	892 (37)	2317 (37)	109 (13)	477 (13)	870 (52)	2215 (56)
121 (1)	500 (171)	1181 (22)	2321 (22)	115 (0)	481 (6)	1149 (25)	2220 (0)
134 (21)	502 (7)	1191 (3)	2327 (3)	131 (22)	486 (29)	1158 (3)	2224 (4)
155 (1)	510 (77)	1204 (0)	2362 (0)	149 (1)	493 (13)	1172 (2)	2267 (236)
192 (0)	516 (10)	1205 (19)	2909 (19)	185 (0)	494 (22)	1173 (12)	2687 ^b
227 (2)	524 (14)	1385 (398)	3614 (398)	217 (2)	498 (11)	1351 (1)	3514 (359)
231 (0)	525 (53)	1390 (40)		222 (0)	507 (49)	1355 (304)	
235 (1)	534 (11)	1399 (16)		225 (1)	511 (94)	1358 (29)	
255 (1)	542 (2)	1413 (1)		244 (1)	515 (4)	1368 (1)	
258 (5)	546 (0)	1431 (72)		248 (4)	518 (1)	1417 (61)	
281 (1)	551 (8)	1462 (167)		268 (1)	521 (0)	1419 (204)	

^a Three very low frequencies have been omitted from the list. ^b Unphysical IR intensity omitted (>5000 km/mol). This is possibly due to a nearby Hartree–Fock orbital instability.

TABLE 7: Harmonic Vibrational Frequencies (cm⁻¹) and IR Intensities (km/mol, in Parentheses) for Dimer 3 (C_{2h} Symmetry), Predicted Using the DZP B3LYP and BP86 Methods^a

B3LYP				BP86			
a _g	b _g	a _u	b _u	a _g	b _g	a _u	b _u
48 (0)	51 (0)	28 (0)	53 (7)	45 (0)	49 (0)	27 (0)	53 (6)
68 (0)	77 (0)	76 (1)	103 (2)	64 (0)	74 (0)	72 (1)	97 (2)
103 (0)	82 (0)	115 (13)	108 (10)	97 (0)	78 (0)	111 (12)	103 (7)
114 (0)	150 (0)	137 (2)	179 (8)	109 (0)	144 (0)	133 (0)	168 (15)
152 (0)	231 (0)	234 (6)	202 (145)	139 (0)	221 (0)	225 (5)	217 (94)
194 (0)	250 (0)	238 (0)	263 (49)	169 (0)	240 (0)	227 (0)	261 (99)
275 (0)	428 (0)	428 (1)	439 (5)	260 (0)	410 (0)	410 (0)	425 (15)
429 (0)	455 (0)	460 (0)	475 (158)	381 (0)	435 (0)	439 (0)	461 (46)
443 (0)	523 (0)	523 (21)	478 (2)	430 (0)	500 (0)	499 (18)	461 (1)
477 (0)	549 (0)	549 (7)	488 (96)	460 (0)	519 (0)	519 (4)	472 (184)
484 (0)	552 (0)	552 (1)	489 (2)	462 (0)	524 (0)	525 (0)	477 (16)
501 (0)	734 (0)	734 (0)	521 (281)	471 (0)	695 (0)	695 (0)	516 (36)
516 (0)	752 (0)	752 (1)	542 (0)	497 (0)	710 (0)	710 (0)	538 (988)
545 (0)	1274 (0)	1272 (148)	796 (5)	524 (0)	1336 (0)	1333 (120)	762 (5)
796 (0)			877 (184)	754 (0)			847 (1022)
868 (0)			880 (5)	771 (0)			863 (37)
887 (0)			1196 (9)	863 (0)			1120 ^b
1190 (0)			1201 (530)	961 (0)			1164 (46)
1197 (0)			1244 (2101)	1165 (0)			1196 (2731)
1216 (0)			1386 (367)	1170 (0)			1361 (137)
1379 (0)			1407 (246)	1362 (0)			1371 (15)
1410 (0)			1483 (29)	1368 (0)			1435 (1)
1484 (0)			1488 (419)	1434 (0)			1443 (440)
1486 (0)			1526 (33)	1436 (0)			1466 (28)
1526 (0)			2130 (3854)	1467 (0)			1571 ^b
2092 (0)			2316 (393)	1530 (0)			2215 (63)
2310 (0)			2320 (47)	2213 (0)			2217 (44)
2318 (0)			2322 (1157)	2216 (0)			2225 (102)
2321 (0)			2326 (120)	2224 (0)			2241 (2530)
2326 (0)			2541 ^b	2225 (0)			2286 (3914)
2470 (0)				2283 (0)			

^a One very low frequency has been omitted from the list. ^b Unphysical IR intensities omitted (>5000 km/mol). These are possibly due to a nearby Hartree–Fock orbital instability.

curve along the N···H stretching coordinate for dimer 1, computed by freezing positions of the acid 1 monomers and computing single-point DZP B3LYP energies as the hydrogen is displaced from its equilibrium position. The result is an asymmetric potential, with no clearly defined maximum or second minimum. The absence of a second minimum, corresponding to PCCp⁻···H⁺–PCCp–H, was confirmed by explicit geometry optimizations, all of which fall back to the minimum shown in Figure 8, indicating the tendency of PCCp–H to not bind a second proton. The symmetrical nature of this potential as defined for a SSLB bond⁶ is not explicit; however, in the actual polymer the potential should be much more symmetric, consistent with the experimental findings, since the proton transfer can be propagated down the chain to prevent the buildup of positive charge on any single PCCp–H moiety:



Predicted vibrational frequencies are included in Tables 6 and 7 for dimers 1 and 3, respectively. It should be noted that while dimer 1 will have a strong IR absorption around 3500 cm⁻¹, this corresponds to the N–H stretch of the “free” proton (not the hydrogen-bound proton), which will only be present at the end of the chain in the actual polymer and not generally observable spectroscopically. As such, frequencies for both dimer 1 and dimer 3 are consistent with the experimental observations of Richardson and Reed.⁵ It is also interesting that B3LYP predicts the highest b_u vibration at 2541 cm⁻¹, much higher than the analogous BP86 frequency, 2286 cm⁻¹, for dimer 3. A component of this B3LYP mode is a large N–H stretch,

which is not as pronounced in the BP86 dimer 3 structure given the nearly symmetric ($\Delta r = 0.18 \text{ \AA}$) N···H–N arrangement.

Conclusions

While there are no experimental EAs for PCCp, the progression of the electron affinities agrees with prior findings in that the values follow BP86 > B3LYP > BLYP. However, given the favorable performance of these functionals compared to experiment for the electron affinity of the Cp radical,²¹ we expect the theoretical errors to be relatively small. Stabilization of the anion through aromaticity, π -system delocalization, and the electron-withdrawing effect of the five cyano substituents contributes to the large theoretical electron affinity of 5.47 eV (from DZP++ B3LYP).

Computed geometries for the protonated anion show that the structure with the proton attached to the nitrile N, as compared to the structure with the proton attached to a ring carbon, is lower in energy by 6.5 kcal/mol, using the B3LYP method, which agrees well with the 7.0 kcal/mol difference reported by Vianello et al.¹¹ This energy difference is attributed to the preservation of aromaticity, coupled with retention of stabilizing conjugation upon protonation of the nitrile group, compared to direct protonation of a ring carbon, which disrupts such stabilizing effects.

We have also examined potential structures for the dimerization of the conjugate acid, confirming the proposed structure of Richardson and Reed⁵ but also suggesting a self-contained dimer structure, connected via two hydrogen bonds, that should be competitive thermodynamically and kinetically. Predicted vibrational frequencies for both the polymeric structure and the

self-contained dimer are consistent with the spectra of Richardson and Reed.⁵ The resulting picture for the proposed polymer is one of a networked structure with numerous kinks and nearly limitless conformational flexibility.

Acknowledgment. This work is supported by National Science Foundation Grant CHE-0451445. S.E.W. thanks J. M. Pristera for valuable comments and discussions.

References and Notes

- (1) Webster, O. W. *J. Am. Chem. Soc.* **1965**, *87*, 1820.
- (2) Webster, O. W. *J. Am. Chem. Soc.* **1966**, *88*, 3046.
- (3) Chen, E. Y.-X.; Marks, T. J. *Chem. Rev.* **2000**, *100*, 1391.
- (4) Strauss, S. H. *Chem. Rev.* **1993**, *93*, 927.
- (5) Richardson, C.; Reed, C. A. *Chem. Commun.* **2004**, 706.
- (6) Stasko, D.; Hoffmann, S. P.; Kim, K.-C.; Fackler, N. L. P.; Larsen, A. S.; Drovetskaya, T.; Tham, F. S.; Reed, C. A.; Rickard, C. E. F.; Boyd, P. D. W.; Stoyanov, E. S. *J. Am. Chem. Soc.* **2002**, *124*, 13869.
- (7) Burk, P.; Koppel, I. A.; Koppel, I.; Yagupolskii, L. M.; Taft, R. W. *J. Comput. Chem.* **1996**, *17*, 30.
- (8) Koppel, I. A.; Burk, P.; Koppel, I.; Leito, I.; Sonoda, T.; Mishima, M. *J. Am. Chem. Soc.* **2000**, *122*, 5114.
- (9) Tang, Z.; BelBruno, J. J.; Huang, R.; Zhang, L. *J. Chem. Phys.* **2000**, *112*, 9276.
- (10) Johansson, P.; Nilsson, H.; Jacobsson, P.; Armand, M. *Phys. Chem. Chem. Phys.* **2004**, *6*, 895.
- (11) Vianello, R.; Liebman, J. F.; Maksiæ, Z. B. *Chem. Eur. J.* **2004**, *10*, 5751.
- (12) Uchimura, H.; Tajiri, A.; Hatano, M. *Chem. Phys. Lett.* **1973**, *19*, 513.
- (13) Rienstra-Kiracofe, J. C.; Tschumper, G. S.; Schaefer, H. F.; Nandi, S.; Ellison, G. B. *Chem. Rev.* **2002**, *102*, 231.
- (14) Huzinaga, S. *J. Chem. Phys.* **1965**, *42*, 1293.
- (15) Dunning, T. H. *J. Chem. Phys.* **1970**, *53*, 2823.
- (16) Becke, A. D. *J. Chem. Phys.* **1993**, *98*, 5648.
- (17) Lee, C.; Yang, W.; Parr, R. G. *Phys. Rev. B* **1988**, *37*, 785.
- (18) Becke, A. D. *Phys. Rev. A* **1988**, *38*, 3098.
- (19) Perdew, J. P. *Phys. Rev. B* **1986**, *33*, 8822.
- (20) Perdew, J. P. *Phys. Rev. B* **1986**, *34*, 7042.
- (21) Rienstra-Kiracofe, J. C.; Graham, D. E.; Schaefer, H. F. *Mol. Phys.* **1998**, *94*, 767.
- (22) Engelking, P. C.; Lineberger, W. C. *J. Chem. Phys.* **1977**, *67*, 1412.
- (23) Oakes, J. M. PhD Thesis, University of Colorado, Boulder, CO, 1984.
- (24) Kong, J.; White, C. A.; Krylov, A. I.; Sherrill, C. D.; Adamson, R. D.; Furlani, T. R.; Lee, M. S.; Lee, A. M.; Gwaltney, S. R.; Adams, T. R.; Ochsenfeld, C.; Gilbert, A. T. B.; Kedziora, G. S.; Rassolov, V. A.; Maurice, D. R.; Nair, N.; Shao, Y.; Besley, N. A.; Maslen, P. E.; Dombroski, J. P.; Dachsels, H.; Zhang, W. M.; Korambath, P. P.; Baker, J.; Byrd, E. F. C.; Van Voorhis, T.; Oumi, M.; Hirata, S.; Hsu, C. P.; Ishikawa, N.; Florian, J.; Warshel, A.; Johnson, B. G.; Gill, P. M. W.; Head-Gordon, M.; Pople, J. A. *Q-Chem*, version 2.0; Q-Chem, Inc.: Export, PA, 2000.
- (25) Schleyer, P. v. R.; Maerker, C.; Dransfeld, A.; Jiao, H.; Hommes, N. J. R. v. E. *J. Am. Chem. Soc.* **1996**, *118*, 6317.
- (26) Wolinski, K.; Hilton, J. F.; Pulay, P. *J. Am. Chem. Soc.* **1990**, *112*, 8251.
- (27) Dodds, J. L.; McWeeny, R.; Sadlej, A. J. *Mol. Phys.* **1980**, *41*, 1419.
- (28) Ditchfield, R. *Mol. Phys.* **1974**, *27*, 789.
- (29) McWeeny, R. *Phys. Rev.* **1962**, *126*, 1028.
- (30) London, F. J. *Phys. Radium* **1937**, *8*, 397.
- (31) Frisch, M. J.; Trucks, G. W.; Schlegel, H. B.; Gill, P. M. W.; Johnson, B. G.; Robb, M. A.; Cheeseman, J. R.; Keith, T.; Petersson, G. A.; Montgomery, J. A.; Raghavachari, K.; Al-Laham, M. A.; Zakrzewski, V. G.; Ortiz, J. V.; Foresman, J. B.; Cioslowski, J.; Stefanov, B. B.; Nanayakkara, A.; Challacombe, M.; Peng, C. Y.; Ayala, P. Y.; Chen, W.; Wong, M. W.; Andres, J. L.; Replogle, E. S.; Gomperts, R.; Martin, R. L.; Fox, D. J.; Binkley, J. S.; Defrees, D. J.; Baker, J.; Stewart, J. P.; Head-Gordon, M.; Gonzalez, C.; Pople, J. A. *Gaussian 94*, revision C.3; Gaussian, Inc.: Pittsburgh, PA, 1995.
- (32) Meyer, R.; Graf, F.; Ha, T.; Günthard, H. H. *Chem. Phys. Lett.* **1979**, *66*, 65.
- (33) Pierloot, K.; Persson, B. J.; Roos, B. O. *J. Phys. Chem.* **1995**, *99*, 3465.
- (34) Applegate, B. E.; Miller, T. A.; Barckholtz, T. A. *J. Chem. Phys.* **2001**, *114*, 4855.
- (35) Reed, A. E.; Curtiss, L. A.; Weinhold, F. *Chem. Rev.* **1988**, *88*, 899.
- (36) Schleyer, P. v. R.; Jiao, H. *Pure Appl. Chem.* **1996**, *68*, 209.
- (37) Chesnut, D. B. *Chem. Phys.* **1998**, *231*, 1.
- (38) Nyulászai, L.; Schleyer, P. v. R. *J. Am. Chem. Soc.* **1999**, *121*, 6872.
- (39) Abraham, R. J.; Canton, M.; Reid, M.; Griffiths, L. *J. Chem. Soc., Perkin Trans. 2* **2000**, 803.
- (40) Krygowski, T. M.; Cyrański, M. K. *Chem. Rev.* **2001**, *101*, 1385.